# Porous Cu-MOF Nanostructures with Anticancer Properties Prepared by a Controllable Ultrasound-Assisted Reverse Micelle Method

**Malihe Zeraati**
Shahid Bahonar University of Kerman
**Mohammadreza Moghaddam-Manesh**
General Bureau of Standard Sistan and Baluchestan Province, Iranian National Standards Organization
**Sara Hosseinzadegan**
University of Sistan and Baluchestan
**Parya Kazemzadeh**
Lorestan university
**Narendra Pal Singh Chauhan**
Bhupal Nobles' University
**Ghasem Sargazi** ( g.sargazi@gmail.com )
Bam University of Medical Sciences

**Research Article**

**Keywords:** Cu-MOF, characterization, cell viability, anticancer

**Posted Date:** October 27th, 2021

**DOI:** https://doi.org/10.21203/rs.3.rs-966648/v1

# Abstract

The ultrasonic assisted reverse micelle method was used to create Cu-MOF from $Cu(NO_3)_2 \cdot 3H_2O$ and 2,6-pyridine dicarboxylic acid in a 1:1 molar proportion. It has been characterized using FT-IR, XRD, nitrogen adsorption analysis SEM and TEM-EDX. Cu-MOF has anticancer properties against MCF-7 breast cancer cells. Cytotoxicity testing was performed on MCF-7 breast cancer cells using the MTT cell viability assay, and cell proliferation and viability were found to be approximately 24 % higher than the control.


# 1. Introduction

Cancer is, unfortunately, one of the leading causes of death for millions of people worldwide. Cancer biology has made great strides in the last decade, but cancer deaths remain high. [1] Traditional drugs for cancer treatment have limitations such as poor pharmacokinetics, poor biological distribution, and adverse side effects. [2] Chemotherapy is the most commonly used cancer treatment, but it has several drawbacks, the most significant of which are low therapeutic efficiency in the treatment process and side effects on normal cells. [1] Since the 1970s, drug release control in drug delivery has been expanding. [2] Drug delivery systems based on nanoparticles are one of the newer methods in drug delivery systems. Drug delivery systems based on nanoparticles can avoid these issues while also increasing efficiency through targeted drug delivery, controlled release, and drug degradation protection. Metal-organic frameworks (MOFs), d layered double hydroxides (LDHs), graphene oxide (GO), and magnetite are some examples of popular drug delivery systems that use nanoparticles today. [1] Some cases that have been investigated in the use of MOF (organic metal frameworks) as drug delivery systems include excellent surface, thermal and chemical stability, high pore volumes, regular porosity and easy operation. [1, 2] Numerous biological reports have been reported from organic metal frameworks, including inhibition of human glioma cell growth [3], anticancer activity [4–6], and antimicrobial properties [7–9]. One of the MOFs with high biological properties is Cu-MOF.[10–12] It is worth noting that the true nature of the active sites in many MOFs containing metal ions is saturated with the coordination of organic ligands. [13] Cu-MOF has superior antibacterial and anticancer properties. [14, 15] The bactericidal mechanism of Cu-MOF is due to the diffusion of $Cu^{2+}$ ions. In addition, the negative charges of lipoproteins are absorbed into the cell wall, they enter the cell and damage the cell wall, alter the function of the enzymes of the cell wall, or create cell wall holes. [16]

In this paper, we have reported synthesis of Cu-MOF using ultrasonic assisted reverse micelle method and characterized by FT-IR, XRD, SEM and nitrogen adsorption. Anticancer activities against MCF-7 breast cancer cells are also reported.

# 2. Experimental Section

# 2.1 Materials

$Cu(NO_3)_2{\cdot}3H_2O$ and 2, 6 pyridine dicarboxylic acid were purchased from Merck. C□□H□□NaSO□ was purchased from Sigma-Aldrich. Double distilled water (DDW) was used in each experiment.

# 2.2 Method

$Cu(NO_3)_2{\cdot}3H_2O$ (Merck, 98%) and 2, 6 pyridine dicarboxylic acid (Merck, 99%) are mixed with 1:1 mmol dissolved in 25 mL of DDW during the preparation of the samples using the ultrasonic assisted reverse micelle method. The resulting solution was added to a mixture of 0.077 mmol of C□□H□□NaSO□ (Sigma, 99%) and 8 mL of $C_6H_{14}$. The resulting mixture was then stirred for 1 h at 85°C. The resulting solution was placed in the ultrasonic device and exposed to ultrasonic irradiation under optimal conditions, which included an ultrasonic duration of 21 minutes, a power of 175 W, and an ultrasonic temperature of 40°C. Cu-MOF crystals form after 30 minutes and are separated by centrifugation and washed with DMF.

# 2.3 Characterization

The X-ray diffraction (XRD) employed for characterization and determination of the crystalline structure and phases during the synthesis of Cu-MOF. To achieve this aim, a powder X-ray diffractometer (Expert MPD, pananalytical, CuKα = 0.154.6 nm) were used in the range of 2θ = 4 – 30 degree with the step width of 0.05 degree. Scanning electron microscope (SEM, model Em 3200, china KyKy corporation) utilized for investigation of the surface morphology. Fourier transform infrared (FT-IR; SHIMADZU FT8400 spectrometer) with a Bruker- tensor 27 series was utilized for determination of vibrational frequency of the prepared samples in the range of 500 and 4000 $cm^{-1}$. Porosities, surface area and pore textural characteristics of samples were determined by adsorption/desorption measures (BET, Belsorp mini II) at 77K in $N_2$ atmosphere. The absorbance was read by spectrophotometer (BioTek Instruments, Inc., Bad Friedrichshall, Germany).

2.4 **Anticancer activities**: Anticancer activity of Cu-MOF was evaluated using MCF-7 breast cancer cells and the MTT cell viability assay according previously reported methods [17, 18]. MCF-7 cells were isolated from the pleural effusion of a 58-year-old woman with metastatic disease. In pellet culture system consisted of control medium including RPMI 1640, 10% FBS and 100 µL of penicillin G/streptomycin mixtures, cells were cultured for a period of two weeks. During cell culture, cell passaging was performed by trypsinization and washing was by phosphate-buffered saline. The cells with density of $1.2 \times 10^4$ (cells/well) were seeded in 96-well plates and for 24 h incubated in condition of 37°C and 5% $CO_2$. With concentrations of 5, 10, 20, 40, 80, 120 and 200 µg/mL of Cu-MOF, cells were treated for 24 and 48 hours. Then, the medium was then removed and 50 µL/well of MTT solutions (2 mg/mL in PBS) and 150 µL/well of fresh medium were added and incubated for 4 h. Finally, after removing the MTT solutions, to solubilize the formazan crystals, 200 µl of DMSO was added and at 570 nm, the absorbance was read using a spectrophotometer.

# 3. Results And Discussion

SEM and TEM analysis were used to investigate the green Cu-MOF morphology, as shown in Fig. 1 and 2. Cu-MOF morphology was spherical or octahedral, and the average particle size distribution is less than 100 nm.[19] As a result, the anticancer properties of the sample were investigated. Fig. 3 depicts the phase formation and purity of the samples as determined by X-ray diffraction. The sample pattern belongs to Cu-MOF, the peaks marked with a circle at 31°, 37°,43°, 52°, 59°, and 77 ° for Cu-MOF (JCPDS**01-072-0075)** [20, 21].

The FTIR spectrum of Cu-MOF is depicted in Fig. 4. Surface water exhibits the structure and hydroxyl bond of the Cu-MOF structure in the 3358 $cm^{-1}$ band. [19, 22] The C=O vibration in Cu-MOF is responsible for the peaks ranging from 2355 $cm^{-1}$ to 2099 $cm^{-1}$ and 1632 $cm^{-1}$. [16] and COO as CA vibration in Cu-MOF [23], respectively. The strong absorption peaks at 1095, 1152 and 1632 $cm^{-1}$ corresponds to the asymmetric and symmetric C-O stretching [24, 25]. Absorption bands between 872 and 995 $cm^{-1}$ can react with symmetric and asymmetric stretching vibrations of C-H [26, 27]. The peaks observed between 451 and 616 are attributed to Cu-O stretching in Cu-MOF [27, 28]. According to the FTIR spectrum, the final structures of Cu-MOF nanostructures are suggested in Fig. 5.

The porous structure of Cu-MOF at 77K is shown in Fig. 5 by nitrogen adsorption/desorption results. Fig. 6 depicts isotherms of the type (I) in the IUPAC classification, which is an example of microporous materials. [29] The early isotherm's dramatic increase and high $N_2$ uptake indicate a high proportion of microporous. Furthermore, the amount of micro/mesoporous is very low because the samples' isotherms in the high pressure region show no obvious hysteresis and tail. [30] In addition, the calculated $N_2$ adsorption/desorption isotherms were related to textural parameters. The surface area of Cu-MOF measured using BET analysis was 284.94 $m^2/g$. As a result, the high surface area and porosity of this sample are determined by N2 uptake by Cu-MOF.

Cu-MOF cytotoxicity was tested on MCF-7 breast cancer cells and the results are shown in Fig. 6. Based on the results of Fig. 7, after 48 h with high concentrations of Cu-MOF (200 g/mL), cell proliferation and viability were observed to be approximately 24 % higher than the control. The $IC_{50}$ value for exposure of Cu-MOF at 24 h, 131 µg/mL was obtained and following at 48 h, 109 µg/mL was obtained. Therefore, breast cancer cell survival was dependent on concentrations of Cu-MOF and time of incubation.

# Conclusion

Cu-MOF was prepared using UARM method and it was further characterized by FT-IR, XRD, SEM and nitrogen adsorption/desorption analysis. It has shown reasonably good anticancer activities against MCF-7 breast cancer cells. In summary, the synthesized Cu-MOF exhibited anti-cancer properties against MCF-7 breast cancer with an $IC_{50}$ value of 109 µg/mL in 48 hours and viability about 24% with the highest test concentration (200 µg/mL) was obtained at 48 h.

# Declarations

**Author Declarations section:** The manuscript is in compliance with ethical standards.

o Ethics approval and consent to participate: We confirm all relevant ethical guidelines have been followed, and any necessary IRB and/or ethics committee approvals have been obtained.

All methods were used in accordance with relevant guidelines and regulations. Also, we confirmed that all experimental protocols were approved by the Ethics Licensing Committee of the Bam University of Medical Sciences (no. 06 on 17/03/2021). In addition, informed consent was obtained from all study participants.

o Consent for publication: In accordance with the copyright transfer or open access rules.

o Availability of data and materials: The datasets used and/or analyzed during the current study available from the corresponding author on reasonable request.

o Competing interests: There is no competing interests.

o Funding: There is no specific funding.

o Authors' contributions

**Malihe Zeraati:** Methodology, Software, Writing- Original Visualization, Writing-

**Mohammadreza Moghaddam-Manesh:** Methodology, Software, Visualization,

**Sara Hosseinzadegan:** Writing- Reviewing and Editing Investigation.

**Parya Kazemzadeh:** Writing- Reviewing and Editing Investigation

**Narendra Pal Singh Chauhan**: Conceptualization, Methodology, Software, Writing- Original, Visualization, Writing- Reviewing and Editing Investigation, Data curation, Validation, Supervision.

**Ghasem Sargazi**: Conceptualization, Methodology, Software, Writing- Original, Visualization, Writing- Reviewing and Editing Investigation, Data curation, Validation, Supervision.

o Acknowledgements: The authors would like to acknowledge from the Bam University of Medical Sciences.

o Disclosure of potential conflicts of interest: The authors declare that they have no conflict of interest.
o Research involving Human Participants and/or Animals: Not applicable.

o Informed consent: Not applicable.

# References

[1] M. Pooresmaeil, H. Namazi, Facile preparation of pH-sensitive chitosan microspheres for delivery of curcumin; characterization, drug release kinetics and evaluation of anticancer activity, International journal of biological macromolecules, 162 (2020) 501-511.

[2] L.-L. Sun, Y.-H. Li, H. Shi, A ketone functionalized Gd (III)-MOF with low cytotoxicity for anti-cancer drug delivery and inhibiting human liver cancer cells, Journal of Cluster Science, 30 (2019) 251-258.

[3] Y.-J. Hu, Y.-M. Li, K. Zheng, W.-H. Zhang, Y.-L. Liu, H. Yang, Construction of a Zn (II)-containing MOF for highly selective detection of picric acid and inhibition of human glioma cell growth, Journal of Molecular Structure, 1202 (2020) 127359.

[4] J. Huang, X.-Y. Pu, Z. Liu, X.-Y. Cao, J. Fu, A 2-Fold Interpenetrating Zn (II)-MOF: Sensitive Detection of Fe 3+ Ion and Anti-Cancer Activity on Breast Cancer Through high Intensity Focused Ultrasound, Journal of Inorganic and Organometallic Polymers and Materials, 31 (2021) 2209-2217.

[5] Z. Yan, X. Li, Q. Fan, H. Bai, S. Wu, Z.-F. Zhang, L. Pan, A water-stable and biofriendly Zn-MOF with pyrazine decorated pores as 5-Fu delivery system to induce human ovarian cancer cells apoptosis and abrogate their growth, Journal of Molecular Structure, 1204 (2020) 127477.

[6] B.-H. Song, X. Ding, Z.-F. Zhang, G.-F. An, Efficient drug delivery of 5-fluorouracil by a biocompatible Zn-metal–organic framework nanostructure and anti-liver cancer activity study, Journal of the Iranian Chemical Society, 16 (2019) 333-340.

[7] F. Akbarzadeh, M. Motaghi, N.P.S. Chauhan, G. Sargazi, A novel synthesis of new antibacterial nanostructures based on Zn-MOF compound: design, characterization and a high performance application, Heliyon, 6 (2020) e03231.

[8] J. Restrepo, Z. Serroukh, J. Santiago-Morales, S. Aguado, P. Gómez-Sal, M.E. Mosquera, R. Rosal, An antibacterial Zn–MOF with hydrazinebenzoate linkers, Eur. J. Inorg. Chem, 2017 (2017) 574-580.

[9] K. Gwon, I. Han, S. Lee, Y. Kim, D.N. Lee, Novel Metal–Organic Framework-Based Photocrosslinked Hydrogel System for Efficient Antibacterial Applications, ACS applied materials & interfaces, 12 (2020) 20234-20242.

[10] D. Chen, B. Li, L. Jiang, Y. Li, Y. Yang, Z. Luo, J. Wang, Pristine Cu-MOF induces mitotic catastrophe and alterations of gene expression and cytoskeleton in ovarian cancer cells, ACS Applied Bio Materials, 3 (2020) 4081-4094.

[11] Z. Xuan, Y. Zhan, G. Song, B. Liu, Two Cu (II) co-ordination polymers: anti-cancer activity on melanoma by reducing cancer cell proliferation, migration, and invasion ability, Inorganic and Nano-Metal Chemistry, 51 (2021) 239-245.

[12] O. Azizabadi, F. Akbarzadeh, S. Danshina, N.P.S. Chauhan, G. Sargazi, An efficient ultrasonic assisted reverse micelle synthesis route for Fe3O4@ Cu-MOF/core-shell nanostructures and its antibacterial activities, Journal of Solid State Chemistry, 294 (2021) 121897.

[13] R.-Q. Zou, H. Sakurai, S. Han, R.-Q. Zhong, Q. Xu, Probing the lewis acid sites and CO catalytic oxidation activity of the porous metal– organic polymer [Cu (5-methylisophthalate)], Journal of the American Chemical Society, 129 (2007) 8402-8403.

[14] A.S. Pires, J. Batista, D. Murtinho, C. Nogueira, A. Karamysheva, M. Luísa Ramos, B.F. Milne, N.T. Tavares, J. Gonçalves, A.C. Gonçalves, Synthesis, Characterization and Evaluation of the Antibacterial and Antitumor Activity of HalogenatedSalen Copper (II) Complexes derived from Camphoric Acid, Applied Organometallic Chemistry, (2020) e5569.

[15] L. Gu, P. Wang, Q. Zhong, Y. Deng, J. Xie, F. Liu, F. Xiao, S. Zheng, Y. Chen, G. Wang, Copper salt-catalyzed formation of a novel series of triazole–spirodienone conjugates with potent anticancer activity, RSC advances, 7 (2017) 9412-9416.

[16] F. Abbasloo, S.A. Khosravani, M. Ghaedi, K. Dashtian, E. Hosseini, L. Manzouri, S.S. Khorramrooz, A. Sharifi, R. Jannesar, F. Sadri, Sonochemical-solvothermal synthesis of guanine embedded copper based metal-organic framework (MOF) and its effect on oprD gene expression in clinical and standard strains of Pseudomonas aeruginosa, Ultrasonics sonochemistry, 42 (2018) 237-243.

[17] M. Moghaddam-manesh, H. Beyzaei, M.H. Majd, S. Hosseinzadegan, K. Ghazvini, Investigation and comparison of biological effects of regioselectively synthesized thiazole derivatives, Journal of Heterocyclic Chemistry, (2021).

[18] P. Ji, L. Wang, S. Wang, Y. Zhang, X. Qi, J. Tao, Z. Wu, Hyaluronic acid-coated metal-organic frameworks benefit the ROS-mediated apoptosis and amplified anticancer activity of artesunate, Journal of drug targeting, 28 (2020) 1096-1109.

[19] R. Kaur, A. Kaur, A. Umar, W.A. Anderson, S.K. Kansal, Metal organic framework (MOF) porous octahedral nanocrystals of Cu-BTC: Synthesis, properties and enhanced adsorption properties, Materials Research Bulletin, 109 (2019) 124-133.

[20] P.J.A.C. Süsse, Verfeinerung der kristallstruktur des malachits, Cu2 (OH) 2CO3, 22 (1967) 146-151.

[21] R. Riccò, O. Linder-Patton, K. Sumida, M.J. Styles, K. Liang, H. Amenitsch, C.J. Doonan, P.J.C.o.M. Falcaro, Conversion of copper carbonate into a metal–organic framework, 30 (2018) 5630-5638.

[22] J. Lin, D. Wang, D. Chen, Q. Ge, G. Ping, M. Fan, L. Qin, K. Shu, Preparation and enhanced photocatalytic performance of one-dimensional ZnO nanorods, Environmental Progress & Sustainable Energy, 34 (2015) 74-80.

[23] S.B. da Silva, M. Amorim, P. Fonte, R. Madureira, D. Ferreira, M. Pintado, B. Sarmento, Natural extracts into chitosan nanocarriers for rosmarinic acid drug delivery, Pharmaceutical Biology, 53 (2015) 642-652.

[24] S. Lin, Z. Song, G. Che, A. Ren, P. Li, C. Liu, J. Zhang, Adsorption behavior of metal–organic frameworks for methylene blue from aqueous solution, Microporous and mesoporous materials, 193 (2014) 27-34.

[25] F.N. Azad, M. Ghaedi, K. Dashtian, S. Hajati, V. Pezeshkpour, Ultrasonically assisted hydrothermal synthesis of activated carbon–HKUST-1-MOF hybrid for efficient simultaneous ultrasound-assisted removal of ternary organic dyes and antibacterial investigation: Taguchi optimization, Ultrasonics sonochemistry, 31 (2016) 383-393.

[26] S. Liu, L.-H. Fu, Y.-J. Liu, L.-Y. Meng, Y.-Y. Dong, Y.-Y. Li, M.-G. Ma, Cu/C or Cu2O/C composites: selective synthesis, characterization, and applications in water treatment, Science of Advanced Materials, 8 (2016) 2045-2053.

[27] K. Stehfest, M. Boese, G. Kerns, A. Piry, C. Wilhelm, Fourier transform infrared spectroscopy as a new tool to determine rosmarinic acid in situ, Journal of plant physiology, 161 (2004) 151-156.

[28] N.X.D. Mai, J. Yoon, J.H. Kim, I.T. Kim, H.B. Son, J. Bae, J. Hur, Hybrid hydrogel and aerogel membranes based on chitosan/prussian blue for photo-fenton-based wastewater treatment using sunlight, Science of Advanced Materials, 9 (2017) 1484-1487.

[29] J. Rouquerol, F. Rouquerol, P. Llewellyn, G. Maurin, K.S. Sing, Adsorption by powders and porous solids: principles, methodology and applications, Academic press2013.

[30] S. Javanbakht, M. Pooresmaeil, H. Namazi, Green one-pot synthesis of carboxymethylcellulose/Zn-based metal-organic framework/graphene oxide bio-nanocomposite as a nanocarrier for drug delivery system, Carbohydrate polymers, 208 (2019) 294-301.

# Figures

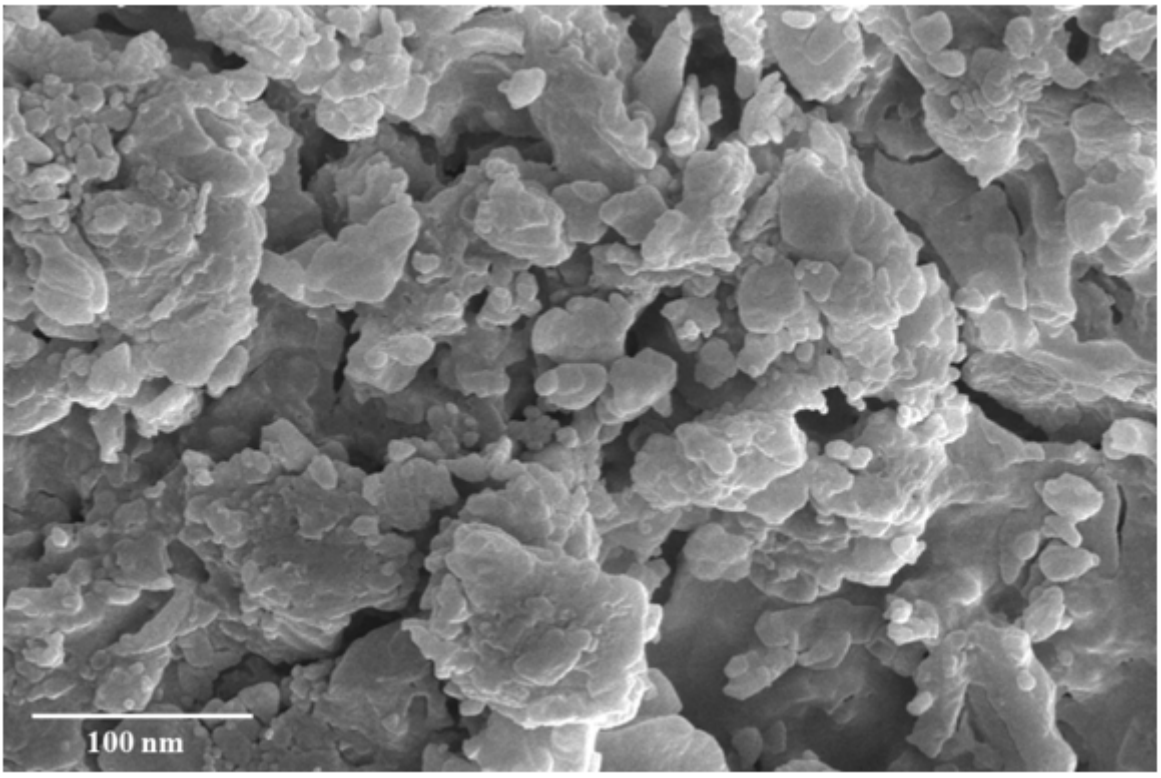


## Figure 1

SEM image of the Cu-MOF.

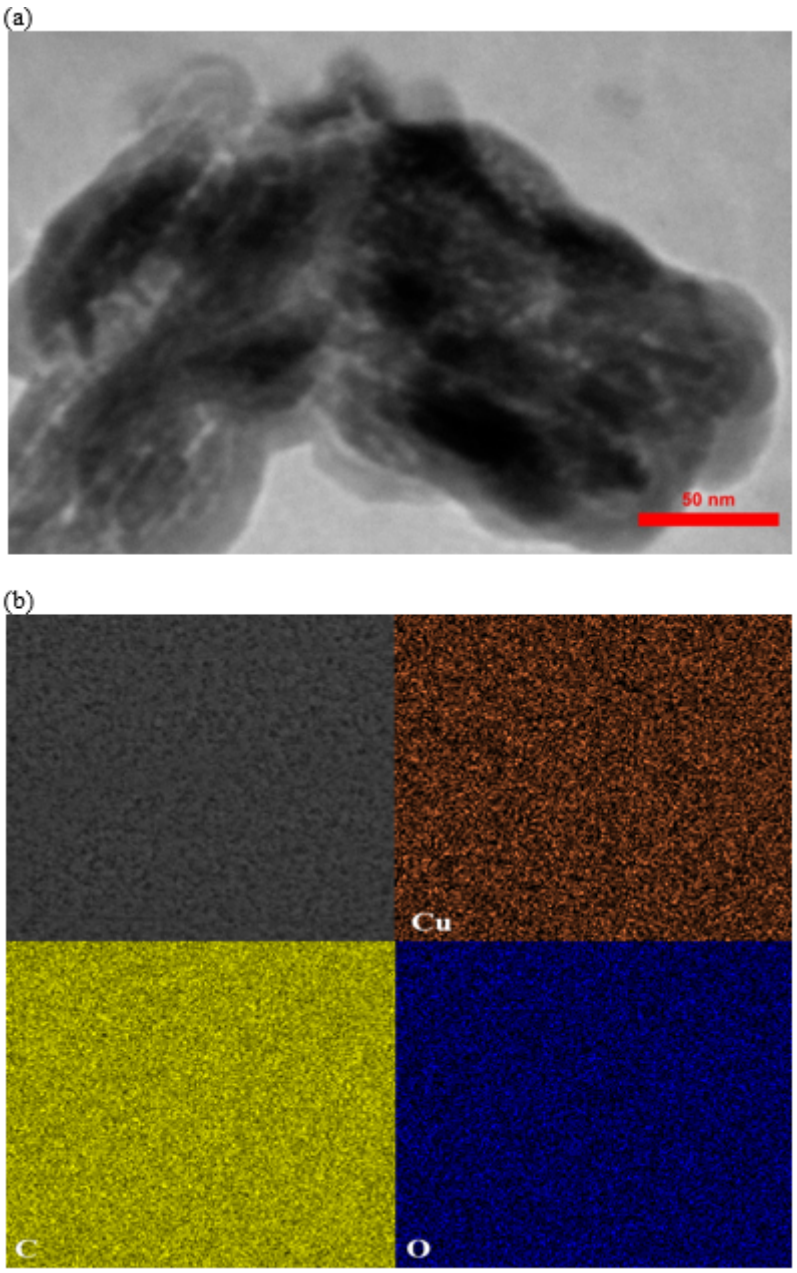


## Figure 2

(a)TEM image of the Cu-MOF and (b)its mapping.

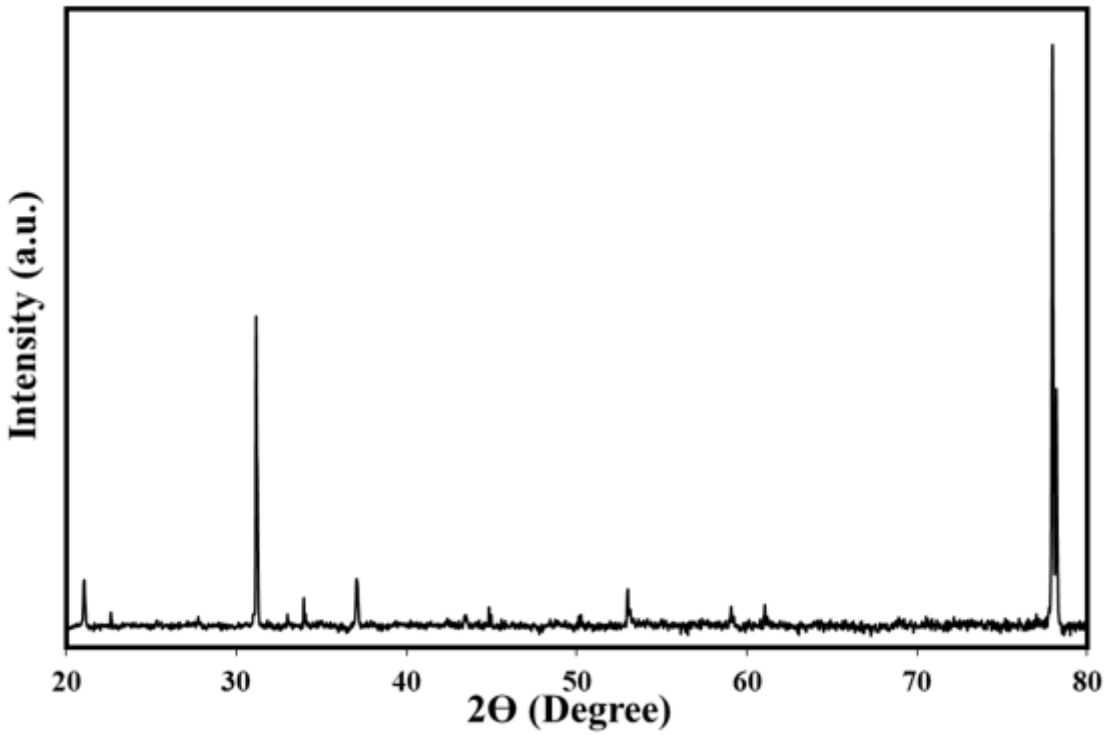


Figure 3

The X-ray diffraction pattern of Cu-MOF.

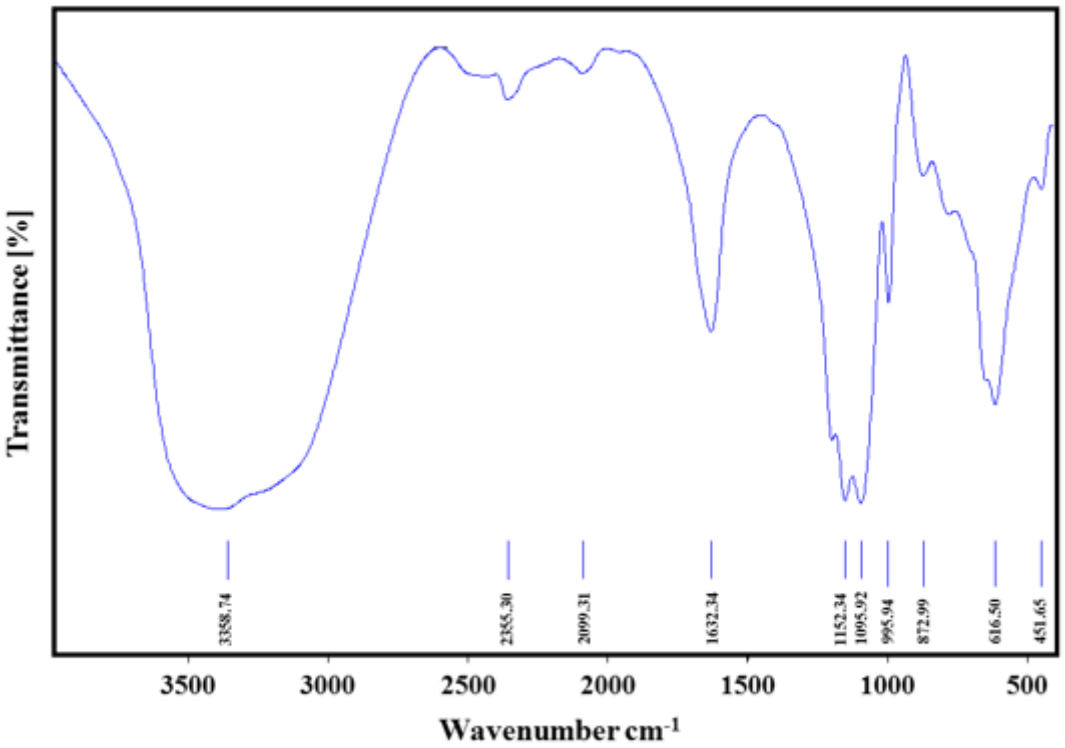


Figure 4

The FTIR spectrum of Cu-MOF.

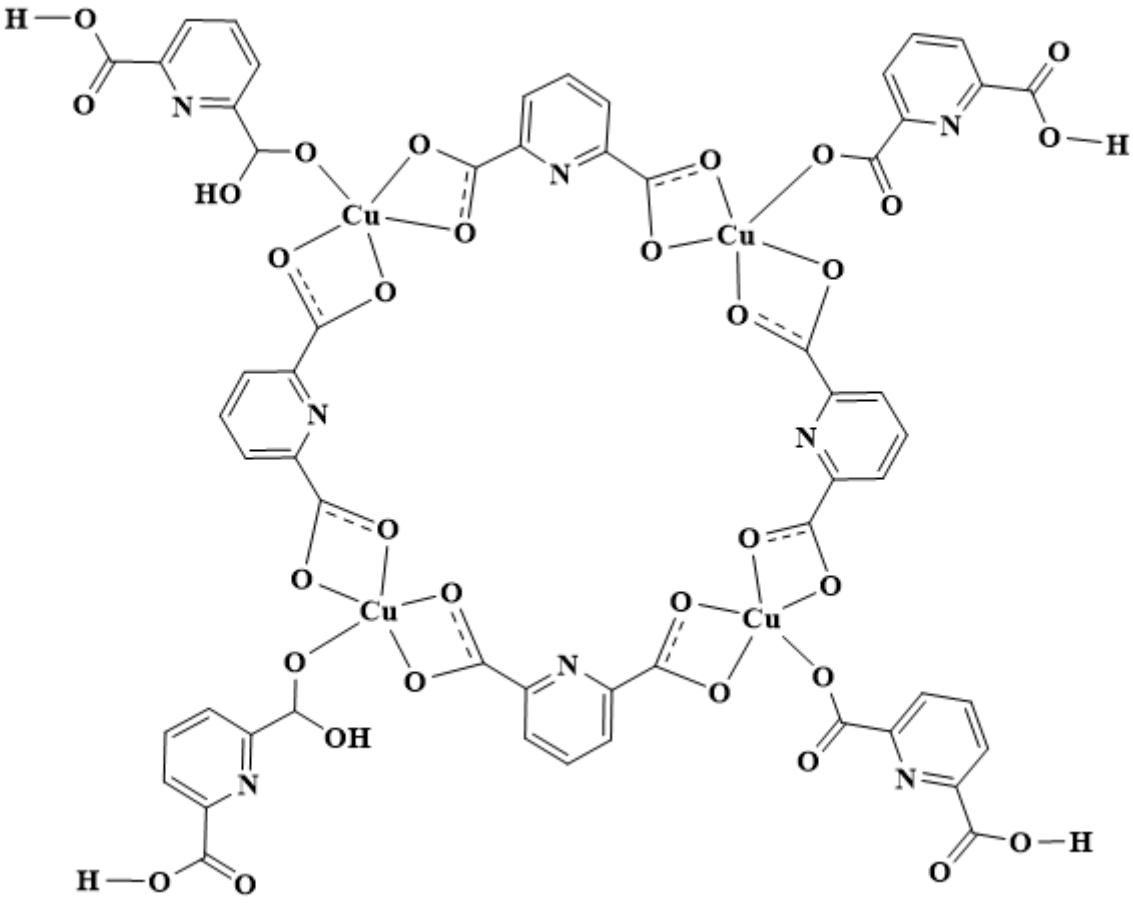


## Figure 5

The proposed structures of Cu-MOF.

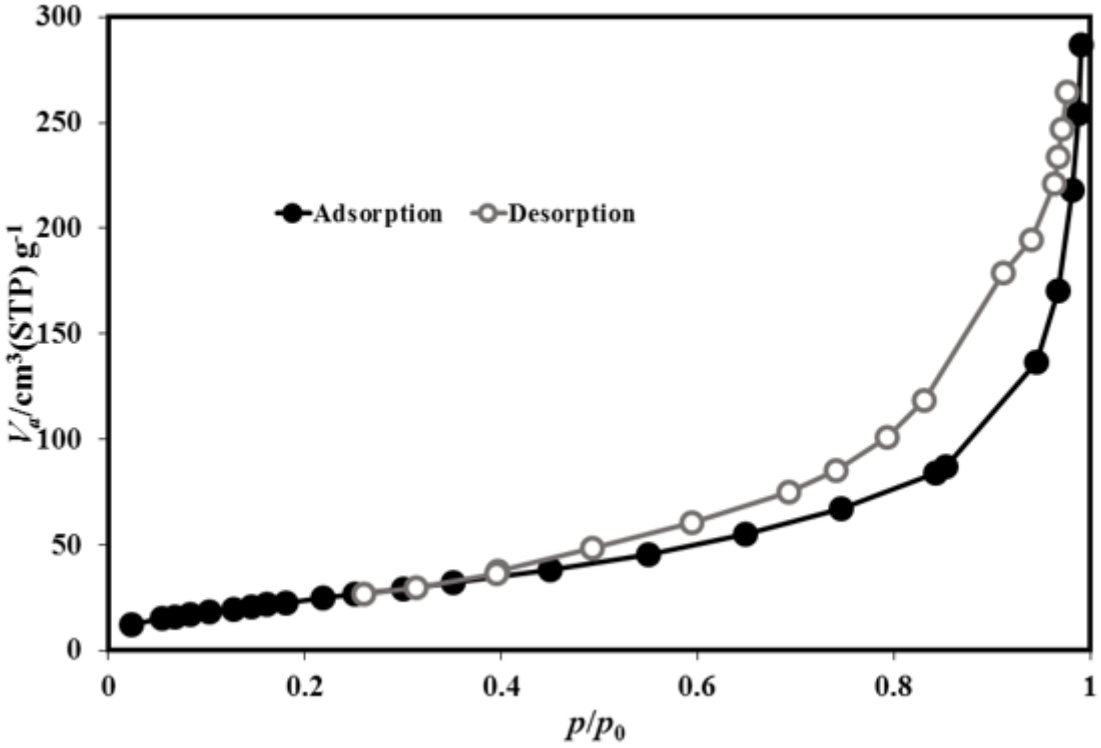


## Figure 6

Nitrogen adsorption desorption curve for Cu-MOF at 77K.

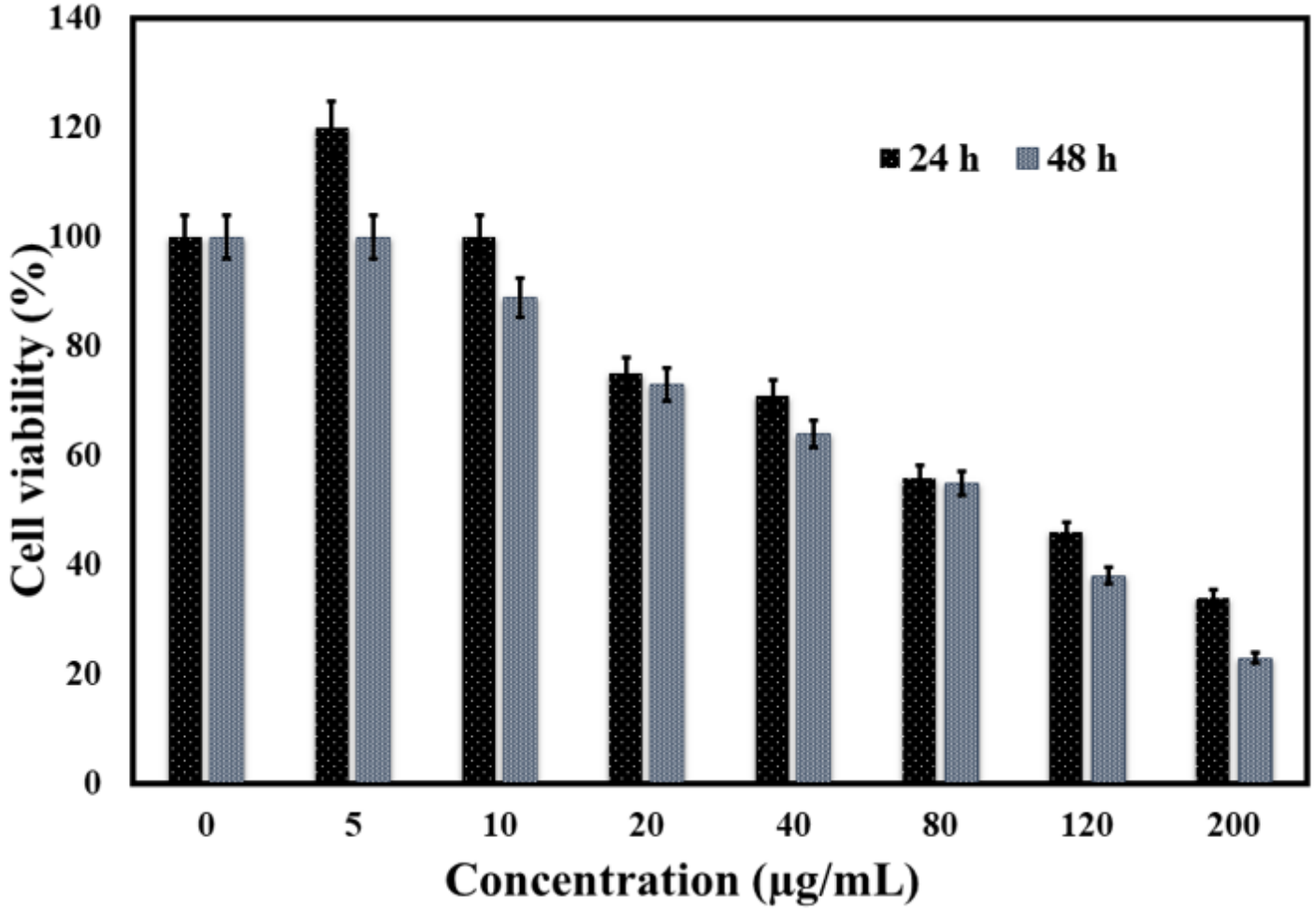


## Figure 7

Anticancer result of Cu-MOF in MCF-7 breast cancer cell for 24 and 48 h. Data represents mean (n = 3) ± SD.